Nucleic Acids Research, 2024, **52**, 10416–10430
https://doi.org/10.1093/nar/gkae674
Advance access publication date: 9 August 2024
Molecular Biology

Transposition with Tn*3*-family elements occurs through interaction with the host β-sliding clamp processivity factor

Yu Tang[1,*,†], Jianfeng Zhang[2,3,†], Jiahao Guan[3,†], Wei Liang[4], Michael T. Petassi[5], Yumeng Zhang[3], Xiaofei Jiang[6], Minggui Wang[2], Wenjuan Wu[1,*], Hong-Yu Ou[3,*] and Joseph E. Peters[5,*]

[1]Department of Laboratory Medicine, Shanghai East Hospital, Tongji University School of Medicine, Shanghai 200123, China
[2]Institute of Antibiotics, Huashan Hospital, Fudan University, Shanghai 200040, China
[3]State Key Laboratory of Microbial Metabolism, Joint International Laboratory on Metabolic & Developmental Sciences, School of Life Sciences & Biotechnology, Shanghai Jiao Tong University, Shanghai 200240, China
[4]Department of Laboratory Medicine, The First Affiliated Hospital of Ningbo University, Ningbo 315010, China
[5]Department of Microbiology, Cornell University, Ithaca, NY 14853, USA
[6]Department of Laboratory Medicine, Huashan Hospital, Shanghai Medical College, Fudan University, Shanghai 200040, China

[*]To whom correspondence should be addressed. Tel: +1 607 255 2271; Fax: +1 607 255 2271; Email: joe.peters@cornell.edu
Correspondence may also be addressed to Yu Tang. Tel: +86 021 3880 4518; Fax: +86 021 3880 4518; Email: tangyu0724@126.com
Correspondence may also be addressed to Wenjuan Wu. Tel: +86 021 2033 4503; Fax: +86 021 2033 4503; Email: wwj1210@126.com
Correspondence may also be addressed to Hong-Yu Ou. Tel: +86 021 3420 4710; Fax: +86 021 3420 4710; Email: hyou@sjtu.edu.cn
[†]The first three authors should be regarded as Joint First Authors.

Abstract

Tn*3* family transposons are a widespread group of replicative transposons, notorious for contributing to the dissemination of antibiotic resistance, particularly the global prevalence of carbapenem resistance. The transposase (TnpA) of these elements catalyzes DNA breakage and rejoining reactions required for transposition. However, the molecular mechanism for target site selection with these elements remains unclear. Here, we identify a QLxxLR motif in N-terminal of Tn*3* TnpAs and demonstrate that this motif allows interaction between TnpA of Tn*3* family transposon Tn*1721* and the host β-sliding clamp (DnaN), the major processivity factor of the DNA replication machinery. The TnpA-DnaN interaction is essential for Tn*1721* transposition. Our work unveils a mechanism whereby Tn*3* family transposons can bias transposition into certain replisomes through an interaction with the host replication machinery. This study further expands the diversity of mobile elements that use interaction with the host replication machinery to bias integration.

Graphical abstract

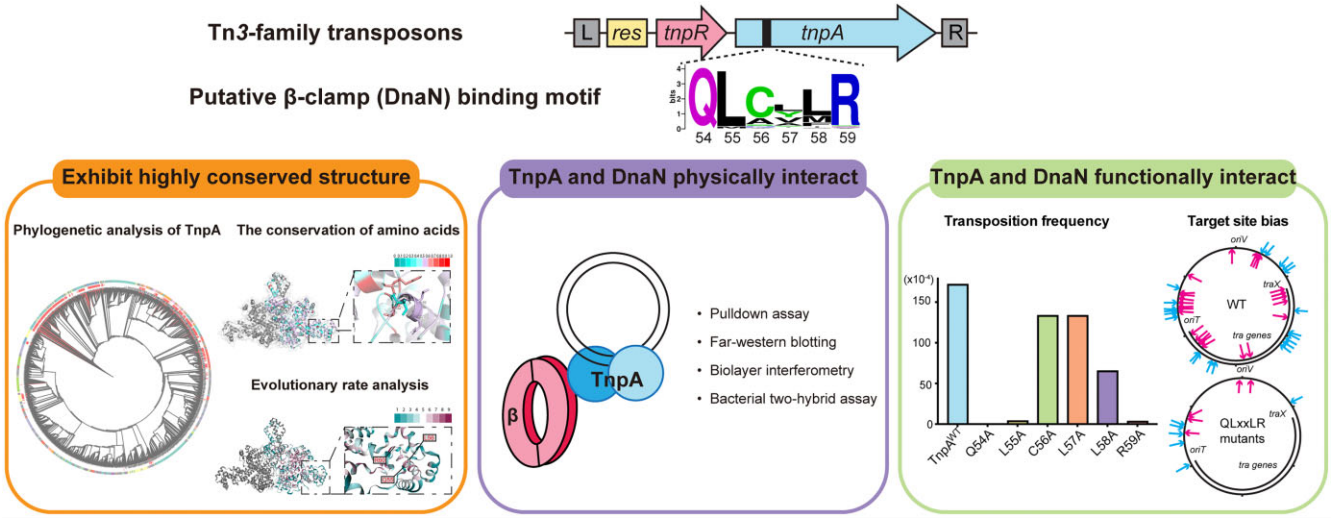

Received: March 1, 2024. **Revised:** July 18, 2024. **Editorial Decision:** July 19, 2024. **Accepted:** July 23, 2024

Introduction

DNA transposition is a common mechanism for horizontal gene transfer allowing a discrete region of DNA called a transposon to move from one location to another within the cell (1). The gene encoding the recombinase that moves transposons, the transposase, has been argued to be one of the most abundant genes in nature, reflecting their important role in accelerating biological diversification and evolution of all forms of life (2).

Tn*3* family transposons are a widespread group of bacterial transposons, known for the variety of passenger genes they mobilize, including genes associated with, beneficial catabolic pathways, virulence determinants, toxin-antitoxin systems, and especially antimicrobial drug resistance (3,4). Several members of the Tn*3*-family (e.g. Tn*4401* and Tn*1721*) are responsible for the global prevalence of *Klebsiella pneumoniae* carbapenemase (KPC)-producing Enterobacterales, regarded as a major threat to public health worldwide (5–7). An intriguing feature of Tn*3*-family transposons is their target site selection bias, which is expected to facilitate their broad distribution. Tn*3*-family transposons preferentially insert into other mobile elements such as phages and plasmids, but especially conjugal plasmids, a targeting feature that is expected to facilitate dissemination of the element to new hosts (8,9). Several members were found to preferentially insert into the region close to the replication origin or termination region where replication forks are predicted to progress slowly or stall. The Tn*4430* transposase also preferentially binds to nicked DNA substrates that mimic a replication fork *in vitro* (10). These findings suggested the Tn3 family transposition machinery may have adapted to specifically target features of DNA replication to promote target site selection. Such interactions have been described for other unrelated mobile genetic elements, including Tn*7*, IS*608* and group II Introns (11–13). The recombinases in these systems have been shown to interact with the β-sliding clamp (DnaN), an essential replication factor that provides processivity to DNA polymerases and coordinates numerous enzymatic activities in the replisome (14,15). Interestingly, interaction between recombination proteins and processivity factors has also been suggested in other domains of life. For example, LINE-1 element mobilization peaks in S phase and utilizes and interaction with the processivity factor PCNA in human cells (16,17).

In this work, we identified a conserved a QLxxLR motif in the N-terminal region of Tn*3* TnpAs which resembles the motif known to accommodate interaction with DnaN. We show that this motif in the TnpA transposase of Tn*1721* is involved in binding β-sliding clamp physically and functionally. Such an interaction is crucial for transposition and likely helps bias transposition into regions associated with DNA replication. Mutations in this motif abolish or drastically reduce transposition. Based on these results, we propose a model to describe a mechanism whereby Tn*3* family transposons can bias transposition to replisomes through an interaction with the host replication machinery.

Materials and methods

Bioinformatics analysis.

Protein sequences were extracted from GenBank-format files of all 26 573 bacterial genomes downloaded from NCBI RefSeq database (18) on 29 May 2021. The profile for the Tn*3*-family transposase (TnpA) (DDE_Tnp_Tn3 domain, PF01256) (19), was used in a hmmsearch (HMMER 3.3.2) (20) (*E*-value < 1e-5) to identify homologs. A total of 15 566 TnpA proteins were identified (Supplementary Dataset S1). After removing duplicates, 3 097 non-redundant TnpA proteins were obtained (Supplementary Dataset S2). Candidate proteins were scanned for the putative DnaN-binding motif, 6 amino acid sequence using FIMO (21) (E-value < 1e-9). Taxonomy information of proteins were obtained from NCBI Taxonomy database (22) using R package rentrez (23). Multiple sequence alignment of proteins was performed using the L-INS-i method in MAFFT v7.481 (24) and visualized by Jalview (25). Phylogenetic trees were constructed using FastTree version 2.1.10 (26) with default parameters and visualized by iTOL (27). Sequence logos of conserved motif was created using WebLogo (28). Tn*3* family transposons were identified using BLASTn search (H-value ≥ 0.8) against sequences in the VRprofile2 database of genes predicted to be in the mobilome (29). 3 653 transposons were obtained in total (Supplementary Dataset S3). Then, 300 base pairs sequences upstream and downstream of these mobilizable transposons were also extracted, and clustered by CD-HIT to remove redundancy (identities ≥ 90%).

Bacterial strains, media and growth conditions

The strains of *Escherichia coli* used for this study are listed in Supplementary Dataset S4, along with a full description of strain source and modification (if any). *E. coli* strains were routinely grown at 30°C or 37°C on LB medium. Antibiotics were added to the medium as required, at the indicated concentrations: 50 μg/ml kanamycin (Kan), at 100 μg/ml ampicillin (Amp), 30 μg/ml chloramphenicol (Cam), 10 μg/ml tetracycline (Tet), 10 μg/ml trimethoprim (Tmp), 10 μg/ml gentamicin (Gen), 20 μg/ml nalidixic acid (Nal) and 100 μg/ml rifampicin (Rif).

Strain construction

A *recA1* version of BW25113 (TYS140) was constructed by P1 transduction using linkage to *srlD3131::Tn10*. The *srlD3131::Tn10* allele can be positively selected with tetracycline resistance and negatively selected using the inability of *srlD* mutants to grow on sorbitol as a sole carbon source. Successful movement of the *recA1* allele is determined by screening UV sensitivity expected with loss of RecA activity.

A FLP expressing *E. coli* host (TYS149) was constructed by cloning the gene expressing FLP into a miniTn7 element, which integrates into the *attTn7* site in the chromosome. The Tn7 delivery plasmid which also expresses the Tn7 transposition machinery was cured at the nonpermissive temperature for the vector (pMS26_FLP (pTY27)) using a previously described procedure (30).

Plasmid construction

Plasmids used in this study are listed in Supplementary Dataset S5, along with the DNA sequences of constructs. Standard molecular cloning techniques were used to make the vectors described below using NEBuilder HiFi DNA assembly master mix (New England BioLabs, USA). Primer pairs and gBlocks used for this study are listed in Supplementary Dataset S6 and Supplementary Dataset S7, respectively. pTY1 was constructed by assembling gBlockA, gBlockB and one PCR product amplified from pVInt (JEP1219 + JEP1220).

pTY2 was constructed by assembling one PCR product amplified from pTY1 (JEP1221 + JEP1222) and one PCR product from pGPS1.1 (JEP1226 + JEP1361). pTY3 was constructed by assembling two PCR products amplified from pTY2 (JEP1221 + JEP1222 and JEP1361 + JEP1362) and one product from pBAD24-FLP (JEP1363 + JEP1364). The *tnpA* expression plasmid, TYS4 was constructed by assembling one PCR product amplified from pBAD322 (JEP1227 + JEP1228) and one PCR product amplified from pHS10842 (JEP1229 + JEP1230, accession number: KP125892.1). QLxxLR mutants of *tnpA* were introduced into pTY4 by assembling two PCR product amplified from pHS10842 (JEP1209 + JEP1524 and JEP1288 + JEP1525, Q54A; JEP1209 + JEP1526 and JEP1288 + JEP1527, L55A; JEP1209 + TP67 and JEP1288 + TP68, C56A; JEP1209 + TP69 and JEP1288 + TP70, L57A; JEP1209 + TP71 and JEP1288 + TP72, L58A; JEP1209 + TP73 and JEP1288 + TP74, R59A) and pTY4 digested with *Eco*RI and *Blp*I. His-tagged transposase expression vectors were constructed by assembling PCR product amplified from pHS10842 (JEP1239 + JEP1288) and cognate plasmid digested with *Pml*I and *Hind*III.

pTY18, pTY19, pTY20 were constructed by assembling one PCR product amplified from pBAD322 (JEP1227 + JEP1228) and one PCR product amplified from pMXB10 (TP107 + TP108, pTY18) or MG1655 (TP103 + TP104, pTY19; TP90 + TP97, pTY20). pTP21, pTP22 and pTP23 were constructed by assembling pET28a digested with *Nco*I and *Blp*I, and one PCR product amplified from pTY4 (TP95 + TP96), MG1655 (TP80 + TP81) and pMXB10 (TP113 + TP114), respectively. pTY24 was constructed by assembling one PCR product amplified from pACYC184 (TP129 + TP130) and one PCR product amplified from pTY21 (TP131 + TP132). pTY25 was constructed by assembling one PCR product amplified from pACYC184 (TP129 + TP130) and one PCR product amplified from pTY22 (TP131 + TP132). pTY26 was constructed assembling one PCR product amplified from MG1655 (TP109 + TP115) and pMXB10 digested with *Nde*I and *Xho*I. pTY27 was constructed by ligating PCR product of FLP amplified from pBAD24-FLP (JEP1450 + JEP1451) into the *Xho*I site of pMS26 following digestion with *Xho*I.

Pulldown assays

Proteins with the Flag-tag were expressed from pET28a in *E. coli* BL21 (DE3), His-tag proteins were expressed from pBAD322 in BW27783. Cells were grown in LB with appropriate antibiotic and 0.2% glucose to OD_{600} of 0.6 and induced with 0.5 mM isopropylthiogalactoside (IPTG) or 0.2% arabinose at 18°C overnight. Aliquots (2 ml) were centrifuged and the pellets were resuspended in 1 ml of lysis buffer (20 mM Tris pH 7.4, 200 mM NaCl). Re-suspended cells were sonicated with four pulses of 10 s each, and were then centrifuged at 12 000 × g for 30 min at 4°C. For His-tagged protein, 80 ul of Anti-His Affinity Gel was added to the supernatant, which was then incubate at 4°C for an hour. The gel was washed three times with lysis buffer and then mixed with the with the supernatant of Flag-tagged proteins, and the resulting mixture was incubated at 4°C for 3 h with gentle shaking. The gel was washed four times and resuspended in 100 μl of LDS sample buffer. The binding of Flag-tagged protein to His-tagged protein was assessed by western blot analysis with anti-Flag rabbit monoclonal antibodies (ABclonal AE063).

Far-western blotting

Far-western blots were performed as described previously (31). The lysate of *E. coli* BL21 (DE3) expressing MBP-Flag (Control) and TnpA-Flag from pTY21 and pTY23 were subjected to SDS-PAGE, and protein bands were bound to the PVDF (Millipore) membranes. The proteins were denatured and renatured as described previously (13). The membrane was blocked for 1 hour at room temperature in Protein Free Rapid Blocking Buffer (EpiZyme, PS108P), and then incubated with DnaN-His (total 5 μg, 1 $\mu g/ml^{-1}$) in the interaction buffer (100 mM NaCl, 20 mM Tris (pH 7.6), 0.5 mM EDTA, 10% glycerol, 0.1% Tween-20, 2% skimmed milk powder and 1 mM DTT) overnight at 4°C. After interaction, the membrane was washed three times with PBST and then incubated with HRP-conjugated monoclonal anti-His antibodies (ABclonal, AE028) in PBST for 2 hours at room temperature. The membrane was washed three times with PBST, and detected using an ECL kit (Tanon), according to the manufacturer's instructions.

Protein purification

His-tagged proteins were purified as described (32). The DnaN protein without a tag was purified using the IMPACT system (NEB) according to the manufacture's recommendations. Proteins were dialyzed in storage buffer before freezing for storage (25 mM Tris [pH 7.5], 200 mM KCl, 10% glycerol).

Biolayer interferometry (BLI)

The affinity of TnpA for DnaN was measured by biolayer interferometry using a ForteBio Octet RED 96 instrument (Fortebio, Fremont, CA, USA). The His-tagged TnpA and MPB (control) proteins (at a concentration of 0.5μM) were immobilized on Ni-NTA biosensors (Fortebio) previously hydrated with running buffer (25 mM Tris [pH 7.5], 150 mM NaCl). Various amounts of DnaN protein (typically 0.5, 1, 2, 3 and 4μM) were used in the association steps. The response was monitored as follows: initial baseline for 60 s, loading for 60 s, association for 180 s and disassociation for 180 s. The Ni-NTA biosensors were regenerated in buffer containing 10 mM glycine pH 1.7, and recharging in 10 mM $NiSO_4$. Each sensor gram was compared with the reference signal obtained for buffer alone at the start of each experiment. Data were analyzed using 1:1 binding stoichiometry, and the equilibrium dissociation constant, KD, was calculated using Octet RED 96 Data Analysis Software version 7.0 (Fortebio).

Bacterial two-hybrid assay

The bacterial two hybrid assay was performed to assess interaction between TnpA and DanN *in vivo* as previously reported with modification (33,34). DnaN was fused to the T25 domain of the *Bordetella* adenylate cyclase and TnpA, QLxxLR mutants, positive control (HolA) and negative control (MPB) were fused to the T18 domain of the *Bordetella* adenylate cyclase. Plasmids encoding fusion proteins were co-expressed in the reporter strain BTH101. Single colonies for each transformation were inoculated into 4 ml of LB medium, respectively, and grown at 37°C, 220 rpm overnight. The culture was adjusted to OD600∼1, and 20 μl culture of each bacterial sample was spotted onto LB agar plates supplemented with kanamycin, ampicillin and X-Gal (40 μg/ml). Plates were

incubated for 8 h at 37°C. In parallel, one milliliter of cells was harvested and subsequently resuspended in 1 ml of Z buffer. β-Galactosidase assays were performed as previously reported (35). β-Galactosidase activity is quantified in units defined as:

$$Miller\ Units = \frac{OD_{420}}{OD_{600} \times\ Time\ (min)} \times\ 1\ 000.$$

The experiments were performed with three biological replicates, each with three parallel independently cultured samples.

Transposition assay

Transposition was monitored with a mini-Tn*1721* element encoded in plasmid pTY3, which also expressed the arabinose-induced FLP recombinase. The mini-Tn*1721* is comprised of the left and right ends of Tn*1721* flanking the kanamycin-resistant gene (Kan) and FLP recognition target (FRT) site. The FRT site recognized by the FLP recombinase was used to allow resolution of cointegrates formed during Tn3 replicative transposition, an efficient site-specific recombinase.

Mating-out transposition assays were performed in BW25142 with pTY3, conjugative plasmid pOX38-Gen, and a derivative of arabinose-induced TnpA expression vector indicated in Supplementary Dataset S5 to monitor transposition frequency and targeting in the conjugative plasmid (See results). Overnight cultures of the donor were subcultured into LB supplemented with appropriate antibiotics at a ratio of 1:100 and transposases expression induced with arabinose or IPTG for approximately three hours. The induced culture were washed twice and mixed with prepared mid-log CW51 recipient strain at a ratio of 1:10 (donor:recipient) and then incubated for 16 hours at 37°C to allow mating. The cultures were collected and then serially diluted in LB 0.2% w/v glucose and plated on LB supplemented with nalidixic acid, rifampicin, gentamycin, with or without kanamycin. Plates were incubated at 37°C for 24 h. The transposition frequency was calculated as the number of Kan^R Gen^R Nal^R Rif^R transconjugants (transposition events) per Gen^R Nal^R Rif^R transconjugant (pOX38-Gen conjugation events).

Mating-in assays were performed to monitor transposition frequency and a preferential targeting across the genome (See results), in which TYS149 with arabinose-induced TnpA expression vector was used as recipient and BW20767 with mini-Tn*1721* plasmid pTY2 was used as donor. The induced recipient strain were mixed with prepared mid-log donor at a ratio of 2:1 (recipient:donor) and incubated on LB supplemented with 0.2% w/v arabinose and rhamnose for 3 h to allow mating. After incubation, cultures were collected and then serially diluted in LB 0.2% w/v glucose and plated on LB supplemented with kanamycin and tetracycline or trimethoprim. Plates were incubated at 37°C for 24 h. The transposition frequency was calculated as the number of Kan^R Tet^R colonies (transposition events) per Kan^R Tmp^R colonies (donor).

Mapping transposition events

Individually isolated CW51 transconjugants from the mate-out assay and BW25113 colonies from mating-in assay with mini-element transposition events were purified on LB supplemented with appropriate antibiotics. Arbitrary PCR and sequencing were performed to capture the position and orientation of transposition events using the exact protocol used previously but with primers specific to this element (36). Primer set R1 (TP13 + TP3, for IRR) and L1 (TP13 + TP6, for IRL) were used for the first PCR. Primer set R2 (TP2 + TP4, for IRR) and L2 (TP2 + TP7, for IRL) were used for the second PCR. TP5 and TP8 were used for sequencing.

Prediction and analysis of transposase structure

The structure of the Tn*4430* (PDB ID: 7QD8) transposase dimer and the dimer complex with DNA (PDB ID: 7QD4) were obtained from RCSB database (37). The prediction of protein structure was achieved via AlphaFold version 2.3.1 (38) with the template of Tn*4430* (PDB ID: 7QD8), running on the Siyuan-1 cluster supported by the Center for High Performance Computing at Shanghai Jiao Tong University with the parameters on Mendeley Data (DOI:10.17632/hnmhh6w2st.4). The conservation of amino acids in Tn*4430* was aligned by clustal omega 1.2.2 (39) and calculated by BLOSUM62 (40). EvoRator (41) was used to predict and visualize site-specific evolutionary rates from protein structures of Tn*4430*, to understand functional regions of the protein. Protein structures and amino acid conservation was visualized using PyMoL (The PyMOL Molecular Graphics System, Version 2.5.5 Schrödinger, LLC).

Results

Bioinformatic analysis of TnpA in Tn*3*-family elements reveals a putative DnaN-binding motif

To support a comprehensive understanding of Tn*3*-family transposons, we conducted a bioinformatics analysis using amino acid sequences of Tn*3* TnpA. Using a HMMER search with Tn*3* TnpA profiles (DDE_Tnp_Tn3, PF01256) (19), we identified 15 566 TnpA protein sequences (Supplementary Dataset S1). After removing duplicates, 3 097 non-redundant TnpA proteins belonging to the Tn*3* family were obtained (Supplementary Dataset S2). In our Supplementary Table S1, the largest percentage of the TnpA proteins was from the Enterobacterales (8 681/15 566, 56%), followed with Pseudomonadales (1 390/15 566, 9%). To a lesser extent, examples were also found in the Burkholderiales, Bacillales, and Lysobacterales, accounting for about 5% of the total. Similarity trees of Tn*3* TnpA sequences supported that this family of elements is widespread in diverse species (Figure 1A and Supplementary Figure S1). An alignment of TnpA proteins revealed a sequence motif in the N-terminal region of TnpA that resembles the QL (S/D)LF motif used for interaction with the sliding clamp protein in bacteria (Figure 1B) (42). We could identify 39 unique peptides with the six-residue motif within this region (Figure 1B). The WebLogo from these 39 examples supported the presence of the QLxxLR motif (Figure 1C). Around 46% (7 161/15 566) of TnpA sequences had examples of this motif (Figure 1D and Supplementary Table S1). The percentages of the motif positive TnpA proteins were highest in Enterobacterales, Pseudomonadales and Aeromonadales, and lower in Burkholderiales, Bacillales, Lactobacillales, Sphingomonadales and Hyphomicrobiales in the available sequenced genomes. The motif was rare in Lysobacterales and Kitasatosporales. Interestingly, the presence of the motif tracks with specific sub-branches supporting the idea that it represents an evolved adaptation within certain lineages of the elements (see discussion).

Additionally, we conducted a BLASTn search (*H*-value ≥ 0.8) using a collection of predicted mobile elements, the

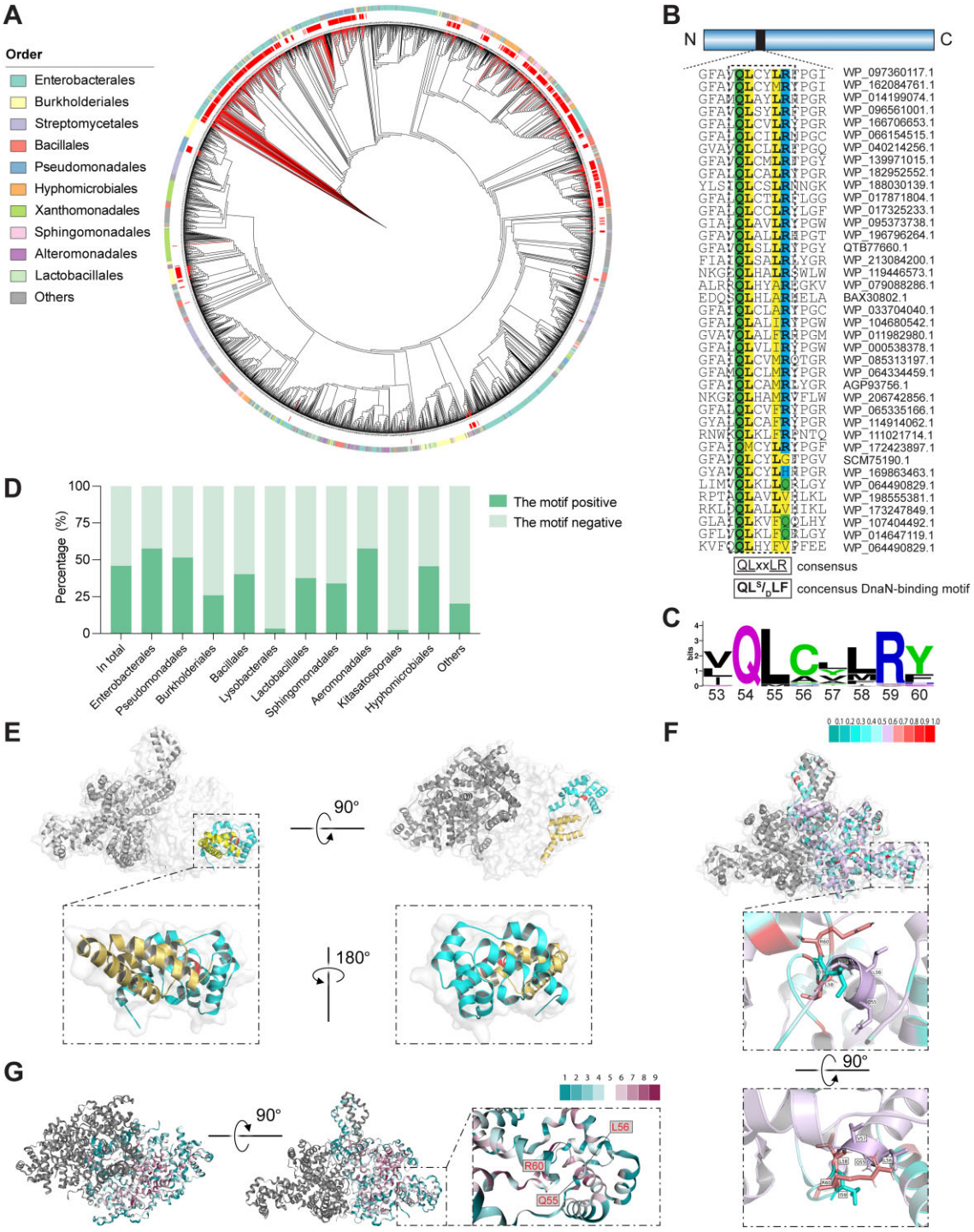

Figure 1. Bioinformatic analysis of Tn*3*-family TnpA proteins reveals a putative DnaN-binding motif. (**A**) Phylogenetic tree of 3 097 non-redundant TnpA proteins belonging to Tn*3* family. The various colors in the outer ring indicate the Order of host strains from which TnpA is identified. Only the top ten Orders are indicated, and the remaining Orders are indicated in light grey. The inner red ring indicates TnpA proteins containing putative β-sliding clamp binding motif, and their lines are also depicted in red. (**B**) An alignment of 39 unique TnpA homologues encompassing the putative β-sliding clamp binding motif is presented with the dashed box. The consensus sequence of the region between residues 54 and 59 containing the putative DnaN-binding motif are shown in bold. Conserved residues within this motif are highlighted in yellow (hydrophobic), green (polar) and blue (positively charged). The consensus DnaN-binding motifs found in bacterial host proteins (QL[S/D]LF) is given for reference. (**C**) Weblogo depicting conserved residues following alignment of DnaN-binding motif. (**D**) Distribution of TnpA proteins with and without the putative β-sliding clamp binding motif in different Orders. (**E**) The structure of Tn*4430* TnpA. The putative DnaN-binding motif and DBD1 were colored as red and cyan, respectively. The arm between DBD1 and DBD2 were indicated in yellow. (**F**) The conservation of amino acids in Tn*3*-family TnpAs. The conservation degree was visualized by gradient colors. The colors ranged from turquoise to red, with red indicating a higher conservation (90–100% identity) and turquoise indicating a lower conservation (less than 10% identity). Additionally, a middle level of conservation (50–60% identity) is indicated by light purple. Close up view of the putative DnaN-binding motif was shown in the lower graphs. (**G**) The site-specific evolutionary rates of Tn*3*-family TnpA. The evolutionary rate of each amino acid of Tn*4430* was gradient colored from turquoise to dark magenta. Higher evolutionary rates were indicated by colors closer to dark turquoise, while lower rates were represented by darker shades of magenta.

VRprofile2 database. This search identified 3 653 Tn*3* family transposons and a screen of non-redundant sequences flanking these transposons indicated at least 1 019 unique integration events (Supplementary Table S2, Supplementary Dataset S8 and Supplementary Dataset S9). Among these non-redundant sequences, more than 60% belong to TnpAs with the QLxxLR motif (636/1 019, 62% for upstream sequences and 930/1 367, 68% for downstream sequences), indicating that these motif-containing TnpAs are actively mobilized. To better understand which instances in the database were from unique insertion events and which where examples where the same integration event was sequenced multiple times, we carried out an additional calculation. We calculated the ratio of the instances of each named transposon to its number of independent insertions to give a sense for the activity in sequenced representatives. In the top five transposons, the ratios of Tn*6016*, Tn*4656*, Tn*6082* and Tn*1* are higher than the average value, suggesting that these transposons may be less active. In comparison, the ratios of several members are less than 2, including Tn*5563*, Tn*3*, Tn*4430*, Tn*1721*, Tn*5422*, etc., implying that these elements are actively moving in nature in the sequenced representatives.

According to recently described cryo-EM structures of Tn*4430* TnpA, the transposase is a dimer (43). We could map the putative DnaN-binding motif to the central helix of DNA-binding domain1 (DBD1) situated between several helices (Figure 1E). To determine whether this motif is conserved in 3D structures of Tn*3* family TnpA proteins, we further predicted the structures of 12 representative transposases from the subgroups of Tn*3* family elements (3) via AlphaFold2 using Tn*4430* as the template. The AlphaFold structures of all 12 TnpA proteins predict a highly similar configuration in the region of the DnaN-binding motif (Supplementary Figure S2). We mapped the conserved amino acids on a 3D structure of Tn*4430* TnpA and found that the putative DnaN-binding motif and the surrounding amino acids were conserved, and that the hydrophilic side chain of R60 extends outward from the DBD1 core, aligning on the surface in a manner analogous to the predicted structure of Tn*1721* (Figure 1F and Supplementary Figure S2). Moreover, an evolutionary rates analysis of amino acids in Tn*4430* TnpA via EvoRator (41) also confirmed the conservation of this motif (Figure 1G). The EvoRato program calculates an evolutionary rate, where a low value indicates that conservation at the position may be due to structural properties, but not a functional interaction. The highly conserved structure and position of this motif imply it might be involved in interacting with DnaN and play an important role in transposition with Tn*3* family elements. Therefore, we hypothesized that Tn*3* TnpA targets structures associated with DNA replication through an interaction with DnaN.

A QLxxLR motif in TnpA facilitates interaction between Tn*1721* TnpA and the host DnaN

Tn*1721* TnpA was tested for a TnpA-DnaN interaction using a pulldown assay with His- and Flag-tagged proteins from cleared lysates from *E. coli* cells. The previously established interaction between the clamp loader subunit HolA and DnaN could be detected (Figure 2A, lane 2), an interaction not seen in the MBP-His control lane (Figure 2A, lane 1). Like the HolA-DnaN control (Figure 2A, lane 2) we identified an interaction between TnpA and DnaN (Figure 2A, lane 3), supporting a model that the TnpA transposase interacts with this important component of the bacterial replisome. We could also detect the previously established DnaN-DnaN and TnpA-TnpA interactions, proteins known to form homodimers (Figure 2A, lanes 4 and 5) (43,44). Consistent with the pulldown assay, we detected a specific signal for His-tagged DnaN at the same molecular weight as the TnpA-Flag, using a far-Western blot (Figure 2B). A signal was not detected in the MBP-Flag negative control lane (Figure 2B). For a quantitative analysis of the TnpA–DnaN interaction, we utilized the biolayer interferometry to test the affinity between TnpA and DnaN. The KD of TnpA-DnaN interaction was determined to be ∼0.29 μM. For comparison, the negative control MBP protein displayed no substantive binding to DnaN (Figure 2C). Together, these results indicate that the TnpA physically interacts with DnaN in multiple *in vitro* assays.

To further test the role of putative QLxxLR motif of TnpA in binding DnaN, we constructed a set of TnpA mutants replacing specific amino acids within this region with alanine and conducted bacterial two-hybrid assay for quantitative analysis. Three TnpA mutants (Q54A, L55A and R59A) were reduced in their ability to interact with DnaN (Figure 2D and E). This was of interest because R59 was predicted to protrude from the surface of TnpA within the DBD1 region (Supplementary Figure S3). Changes at three other amino acid positions (C56A, L57A and L58A) did not appear to influence DnaN binding in our assay. These results support the notion that the conserved QLxxLR motif plays an important role in interacting with DnaN. Albeit, that amino acid changes within this motif show different effects in the static conditions used in this assay. Western blots indicate that changes in stability or expression of TnpA do not account for our finding (see Figure 4A). Together, these results support the view that the conserved QLxxLR motif of Tn*3* TnpA is involved in binding DnaN. Previous studies examining the interactions between DnaN and various bacterial DNA polymerases indicate that the QLxxLR motif interacts with a hydrophobic pocket in DnaN, but that each DNA polymerase will additionally have other interactions with other regions of DnaN. It is expected that TnpA from Tn*3* family elements are likely to have multiple interactions with DnaN in addition to the QLxxLR motif (see discussion).

The QLxxLR motif is required for Tn*1721* transposition *in vivo*

To assess the importance of the TnpA QLxxLR motif for Tn*1721* transposition, we monitored Tn*1721* transposition using a mating-out assay (Figure 3A) comparing TnpA wild type to TnpA mutants. Two mutants (L55A and R59A) displayed transposition frequencies considerably lower than those of the wild-type (WT) control, and transposition could not be detected with the Q54A mutant (Figure 4A). These results indicated that disruption of the DnaN-binding motif in Tn*1721* TnpA either reduced or abolished transposition activity *in vivo*, which matches the decreased DnaN-binding ability found in the assays above measuring the physical interaction between the two proteins. Western blots show that differences in stability or expression of these mutants does not account for the sharp reduction or complete loss of transposition (Figure 4A). The 3D structure prediction also supports the

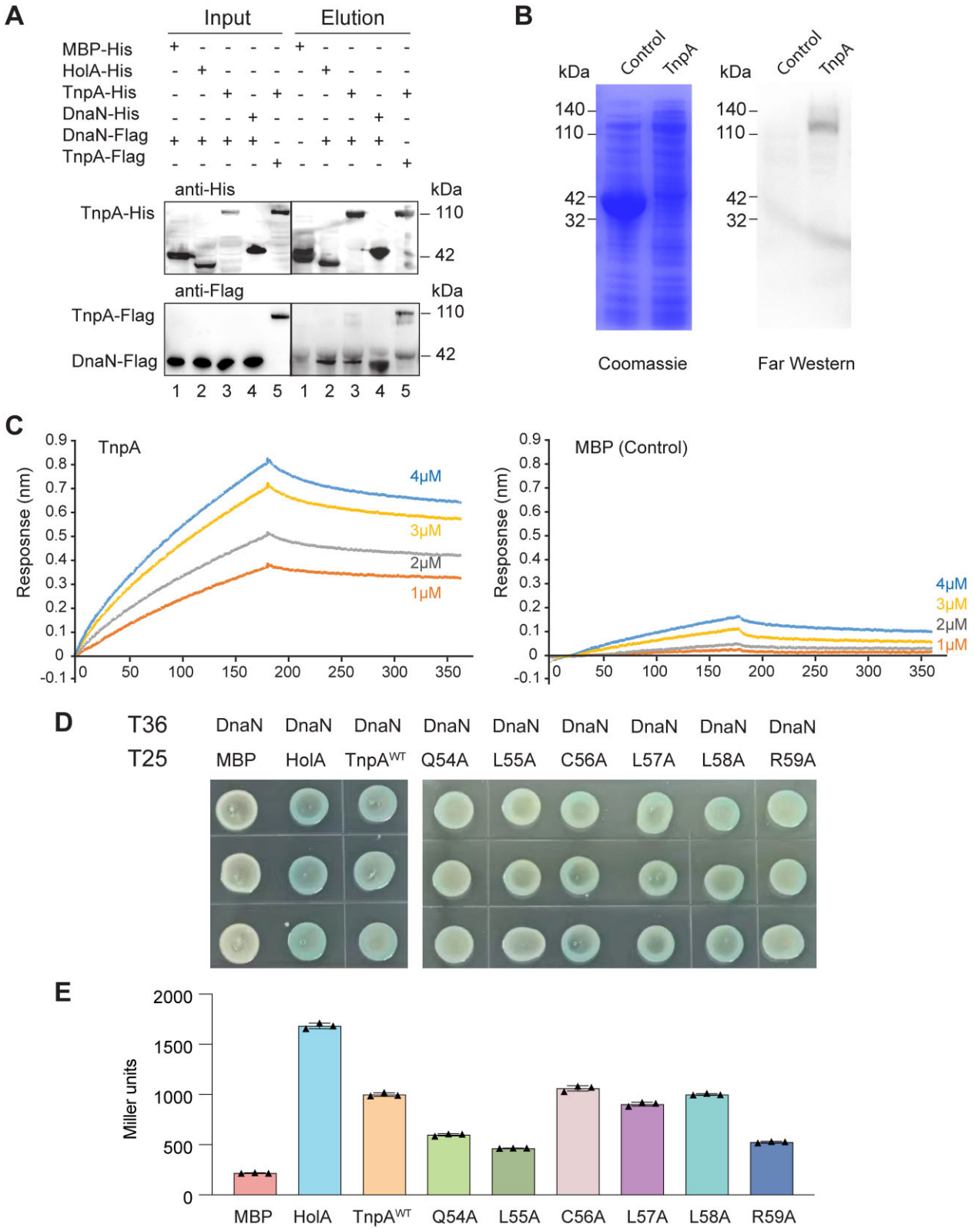

Figure 2. TnpA and DnaN physically interact in both *in vitro* and *in vivo* assays. (**A**) Pulldown assay with TnpA. The His-tagged MBP was used as the negative control, and HolA, the δ subunit of the clamp loader, which has been shown to interact with DnaN in multiple assays, was the positive control. The protein samples of TnpA, MBP and HolA were assayed against supernatants containing Flag-tagged DnaN. Two controls for DnaN-DnaN and TnpA-TnpA interaction were also included to determine whether they were monomers. (**B**) Far western blots. TnpA-Flag retains the signal of His-tag when probed with His-tagged DnaN. The MBP was used as negative control. (**C**) The Biolayer interferometry results for the TnpA (left) and MBP (right). (**D**) Bacterial two-hybrid assay. MBP was used as the negative control and HolA was the positive control. TnpA and TnpA mutants replacing specific amino acids within putative DnaN-binding motif with alanine were also tested. (**E**) Quantitative analysis of DnaN-TnpA interaction using bacterial two-hybrid assay measuring protein activity using the Miller assay. Data indicate mean ± standard deviation ($n = 3$)

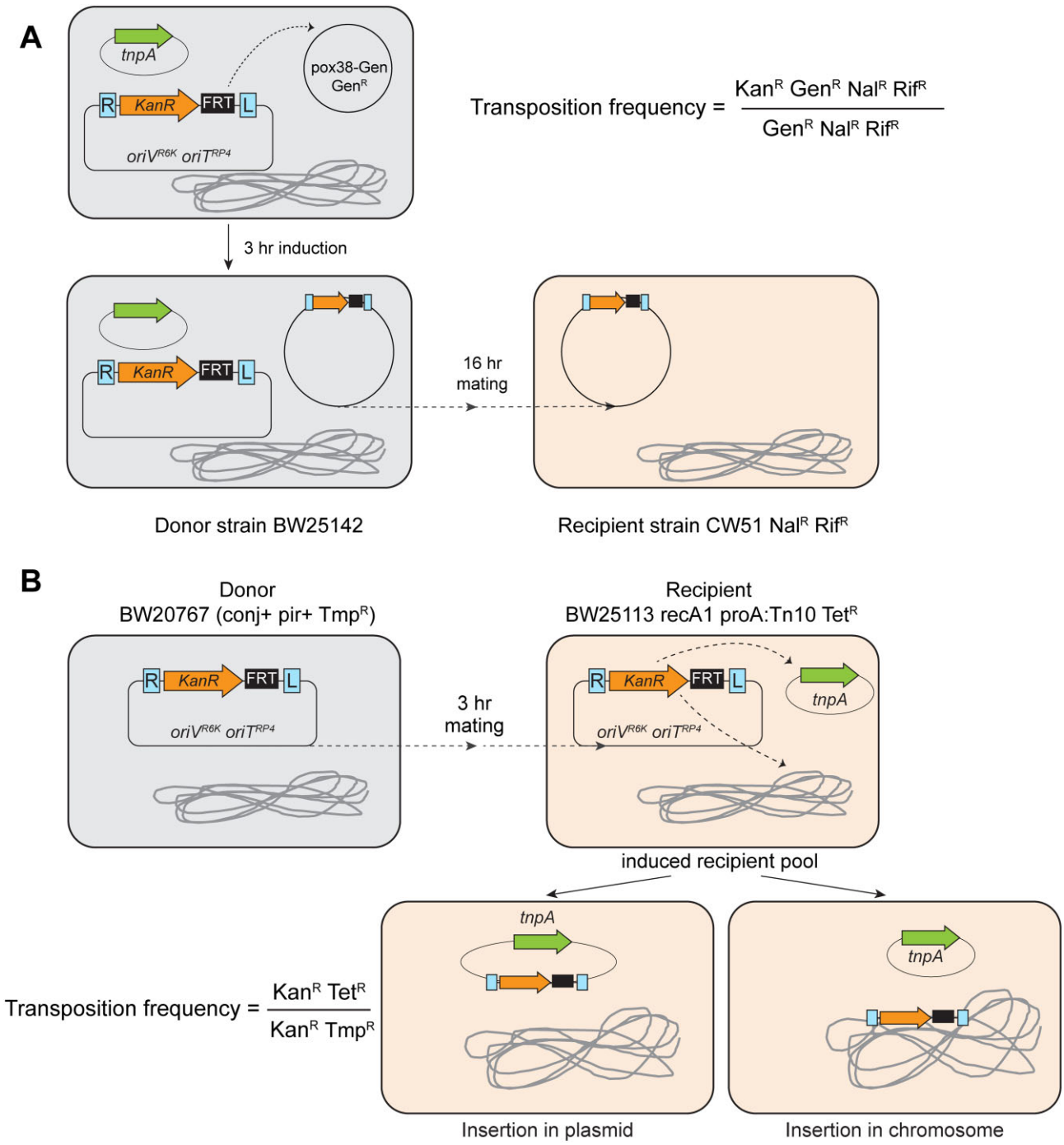

Figure 3. Schematic of *in vivo* transposition assays. (**A**) Mating-out transposition assay. (**B**) Mating-in assay. The process of cointegrate resolution is omitted for simplicity.

idea that the overall structure of the proteins should not be disrupted by these amino acid changes (Supplementary Figure S3). These results indicated that disruption of the putative DnaN-binding motif in TnpA either reduced or abolished transposition activity *in vivo*, which is consistent with the decreased DnaN-binding ability in bacterial two-hybrid assays and the conservation of these sites identified in bioinformatic analysis.

As expected, transposition with the TnpA (Q54A) mutant could be complemented by the co-expression of the TnpA (wt) protein (Figure 4B). Unexpectedly, we found that very low levels of the wild type TnpA protein still would allow a strong dose-dependent increase in transposition with the arabinose induced TnpA (Q54A) mutant (Figure 4B). This result suggests that the TnpA (Q54A) protein which has no transposition activity alone can participate in transposition when expressed with even a low level of leaky expression from the TnpA (wt) vector. To better understand this result, in a follow up assay we kept the expression of the arabinose inducible vector expressing TnpA (Q54A) constant and moni-

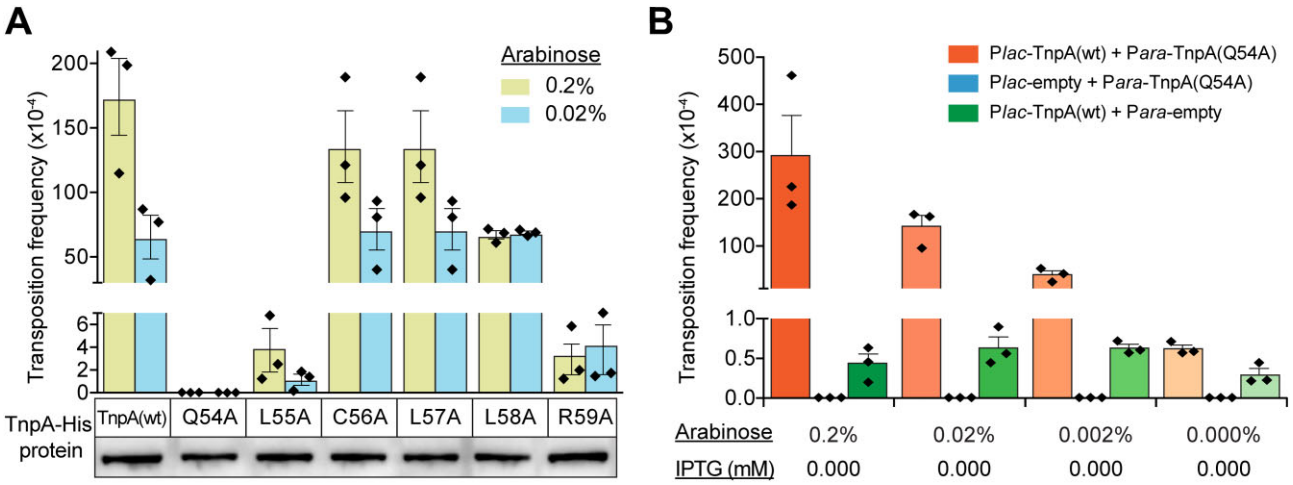

Figure 4. (**A**) Mating-out transposition assay reveals a defect in the ability of TnpA mutants to mediate transposition. Transposition frequency was compromised in the TnpA Q54A, L55A and R59A mutants. All data indicate mean ± standard deviation ($n = 3$). A western blot using an anti-His antibody is displayed below the graph. (**B**) Low level of leaky expression of TnpA (wt) allows TnpA (Q54A) to activate transposition. Transposition was monitored in cells expressing TnpA (Q54A) with *lac*/IPTG control with various arabinose induction levels with TnpA (wt) or an empty vector control. Transposition frequency of Q54A mutant exhibited a dose-dependent rise when complemented with uninduced amounts of TnpA (Q54A). All data indicate mean ± standard deviation ($n = 3$).

tored transposition over a range of TnpA (wt) IPTG induction levels. We conducted the mating-out transposition assay using 0.02% arabinose-induced TnpA (Q54A) and TnpA (wt) was examined at a range of IPTG-induction including the leaky expression found with no induction (Supplementary Figure S4A). In this assay we could again find conditions, where the TnpA (Q54A) protein, that was inactive when tested alone, could participate in transposition with TnpA (wt). This result suggests that the heterodimer of TnpA (Q54A)+TnpA (wt) is functional. One explanation would hold that only one clamp interacting motif is needed in a dimer of TnpA to allow functionality for transposition (see discussion).

We mapped transposition events that occurred into the pOX38-Gen plasmid using arbitrary PCR and Sanger DNA sequencing to determine the junctions around the element (36). By sequencing the junctions where the insertions occurred, we could identify the characteristic 5-bp target site duplication expected with the process of transposition (3,6). As found previously, transposition with TnpA (wt) appeared to occur randomly throughout the pOX38-Gen with insertions occurring in both orientations (Figure 5A) (6). We also mapped integration events that occurred with the TnpA (L55A) and TnpA (R59A) (Figure 5C and D). Sequencing multiple Kanamycin resistant (Kan^R) colonies revealed that almost all of these KanR colonies resulted from just a few independent transposition events. The finding that these were siblings, descendants from just a few independent transposition events, indicated that the frequency of transposition was even lower than predicted by counting Kan^R colonies (i.e. the calculations assumes that Kan^R cells are independent events, but in many instances, they are not). Given the low number of independent transposition events, no claim can be made about the effect of these mutants on target site selection. The TnpA (Q54A) protein does not allow transposition when expressed alone. We mapped transposition events from experiments when TnpA (wt) and TnpA (Q54A) were co-expressed (Figure 5B). Most of the insertions in this experiment were also siblings, but the pattern seemed to resemble the random distribution found with the wild type protein (See discussion).

Tn*1721* exhibits a targeting preference for a plasmid and the terminus region in the chromosome

To characterize any global biases in Tn*1721* transposition we mapped insertions collected from a mating-in assay (Figure 3B). In this assay a conditional delivery vector is used to introduce a mini element into cells. Only cells where transposition occurs out of the delivery vector and into another DNA molecule already in the target cell are selected in the assay. This type of assay provides information about which replicons (plasmid verses chromosome) are preferred and about any targeting biases within the plasmid and chromosomal DNAs. Tn*1721* was found to insert almost exclusively into the transposase expression plasmid (Figure 6). With the integration events we sequenced, 91% (30/33) of the insertions were found in the TnpA expression plasmid. Similar with the findings in mating-out assay, most insertions appeared to be distributed across the entire plasmid (as expected, insertions were not found in the essential origin of DNA replication in the plasmid, pBR322 *Ori*) (Figure 6A). There seemed to be a slight bias for the divergent P_{BAD} promoter region; nine insertions were found distributed across this region (Figure 6A). By contrast, only three insertions were identified in the chromosome. These insertions occurred within a ~25 kb region where clockwise-progressing DNA replication forks are predicted to terminate (Figure 6B). Caution is warranted when drawing conclusions from only a few transposition events, but this result is consistent with the idea that Tn*1721* transposition is also biased to where DNA replication terminates in the bacterial chromosome. Such an integration preference was also found with Tn*917*, another bacterial transposon belonging to Tn*3*-family (36,45). TnpA from Tn*917* also contains a candidate DnaN-binding motif (WP_033704040.1 in Figure 1B).

Architecture of the DnaN binding motif of Tn*3*-family TnpA

To better understand the function of the DnaN-binding motif in transposition, we compared this motif in the TnpA structures of Tn*1721*, Tn*4430* (PDB ID: 7QD8) and Tn*4430*

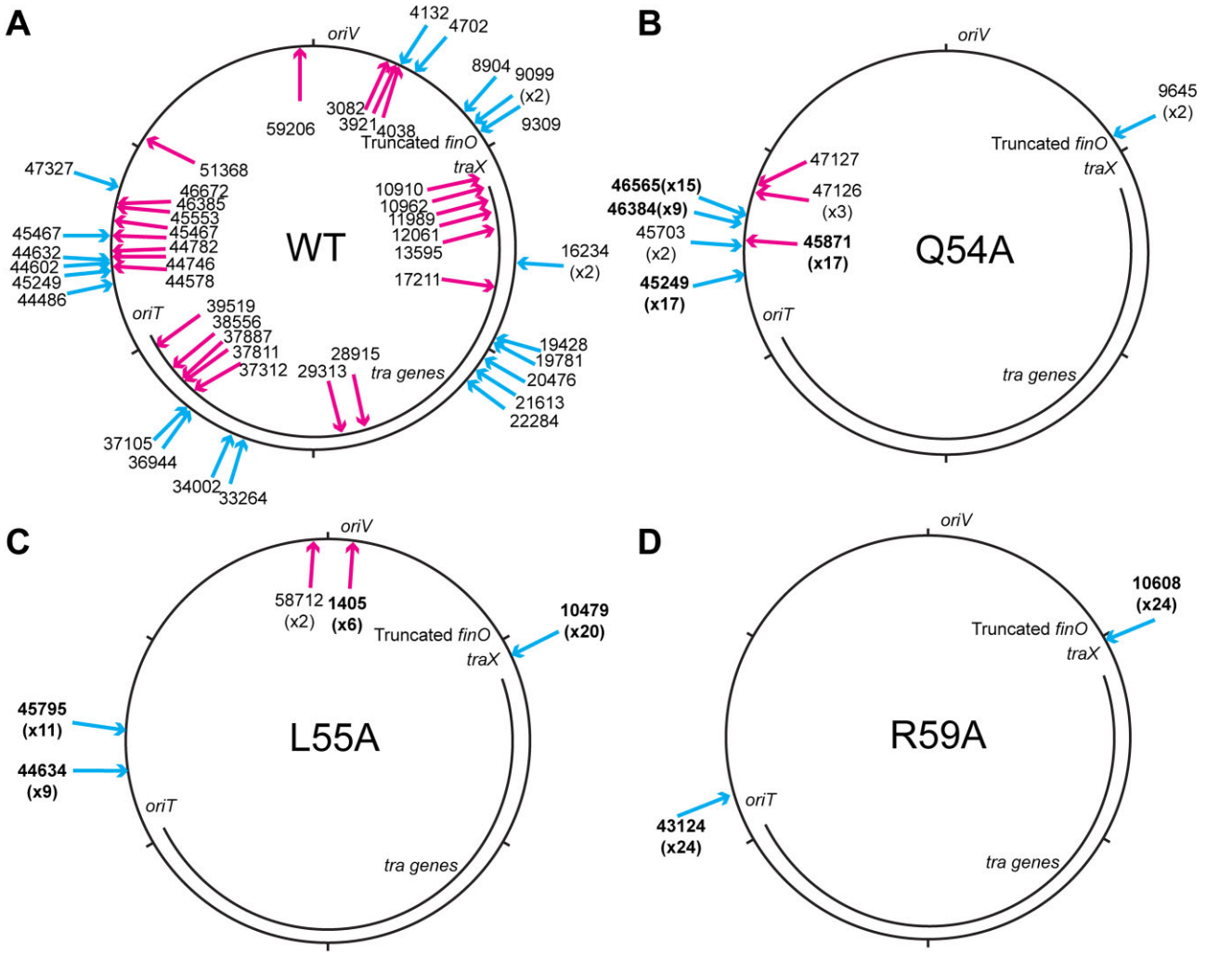

Figure 5. Target site analysis shows that the TnpA-DnaN interaction is needed for efficient transposition into pOX38-Gen. Panels (A–D) indicate the target site of transposition events (arrows) collected in the conjugative plasmid pOX38-Gen mediated by (**A**) TnpA (wt), (**B**) TnpA (Q54A), (**C**) TnpA (L55A) and (**D**) TnpA (R59A). Blue arrows outside the circle indicate insertions of left-to-right orientation; Red arrows inside the circle indicate insertions of opposite left-to-right orientation. Transposition insertions of Q54A group were obtained via co-expression of IPTG-induced TnpA (wt) and arabinose-induced TnpA (Q54A) in Figure 4B.

TnpA-DNA complex structure (PDB ID: 7QD4) (43). The results from the pulldown assay reported above showed that Tn*1721* TnpA is capable of binding DnaN, and such an interaction involves several key amino acids in the conserved QLxxLR motif, including Q54, L55 and R59. Among the amino acids within this motif, only the side chain of arginine [R59 in Tn*1721* ($R59^{Tn1721}$) and R60 in Tn*4430* ($R60^{Tn4430}$)] could extend out from inside of DBD1 to the surface (Figure 7A and B, Supplementary Figure S5A and Supplementary Figure S5B). A similar situation exists in the Tn*4430* TnpA-DNA complex (Figure 7C and Supplementary Figure S5C). Within the conserved QLxxLR motif of Tn*1721* TnpA, the Q54 and L55 in the motif both are sheltered by R59 and two sides of helix structure (Figure 7A and Supplementary Figure S5A).

In order to help identify amino acid residues that are likely conserved due to functional rather than structural constraints, we analyzed the evolutionary rates of amino acids in Tn*4430* TnpA via EvoRator (41). The evolutionary rate of amino acid positions within the protein in DBD1 including the DnaN-binding motif and its neighborhood is very low, while that of the DBD1 surface is substantially higher (Figure 1G and Supplementary Figure S6A-S6F). Most of DNA-binding amino acids including $H104^{Tn4430}$ are located within the region of higher evolutionary rates but not conserved across the Tn*3*-family (Figure 7, Supplementary Figure S6F and Supplementary Figure S7). The DnaN-binding motif with lower evolutionary rates but higher conservation is consistent with our experimental findings that these positions in the DBD1 functions in DnaN binding. We cannot rule out that complete loss of transposition with the Q54A change could result from a combination of loss of DnaN binding and secondary effects on positioning of amino acid H103 for DNA binding (see Discussion). Nevertheless, the QLxxLR DnaN interaction motif that is conserved in specific branches of Tn*3* family element provides a molecular linkage between transposition and DNA replication processes targeted by these elements.

Discussion

Tn*3* family transposons play a critical role in the global spread of important last-resort antibiotics, but basic molecular features that underly how they select target DNAs for integration

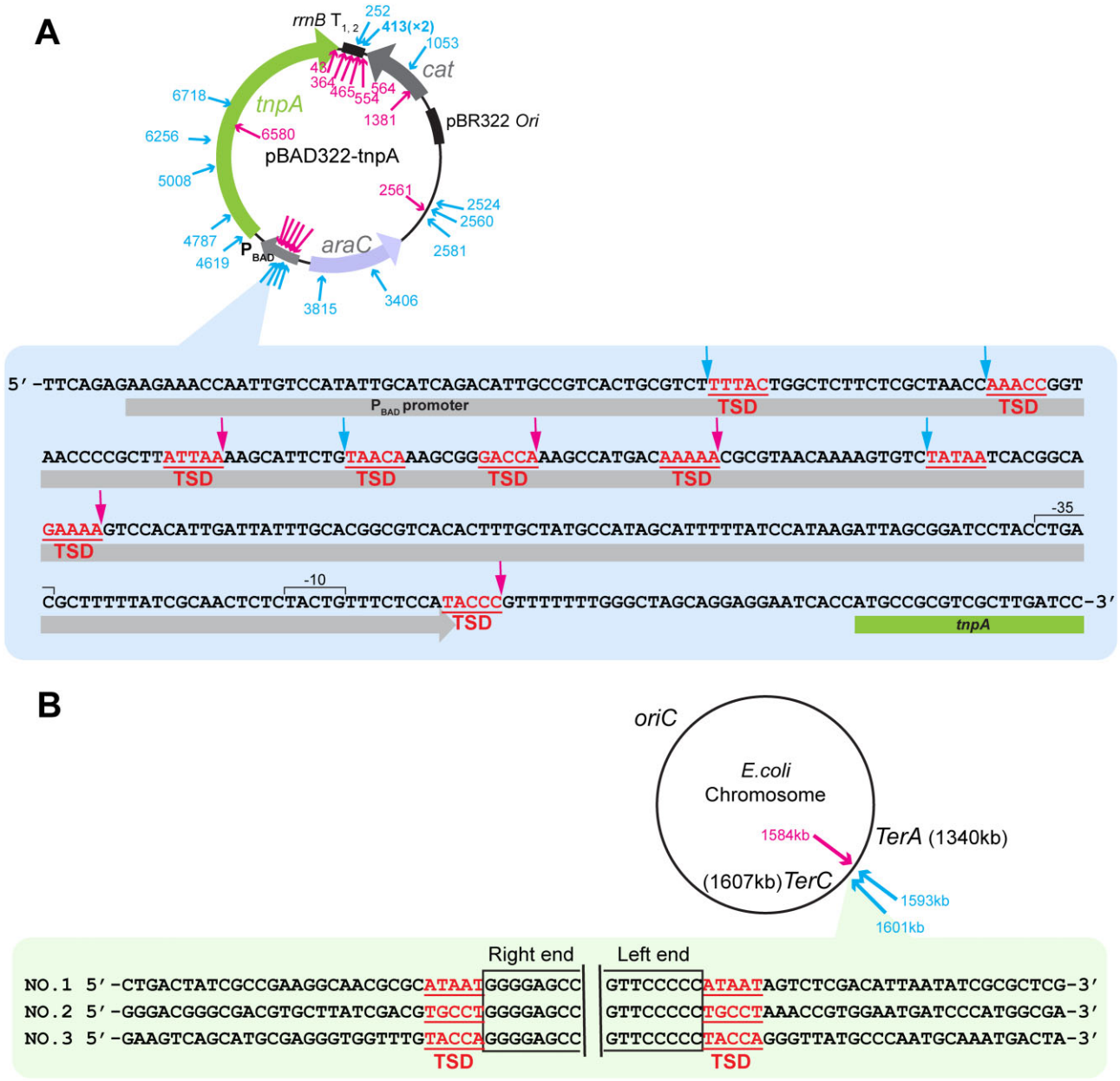

Figure 6. Transposition integration positions and target site duplications (TSD) with transposition events from the mating-in assay. (**A**) Insertions into the pBAD322-*tnpA* plasmid. P_{BAD}, promoter of the L-arabinose operon; *rrnB* $T_{1,2}$, transcription terminator T1 and T2. (**B**) Insertions into the chromosome. Blue arrows outside the circle indicate insertions of left-to-right orientation; red arrows inside the circle indicate insertions of opposite left-to-right orientation.

have remained enigmatic. Here we report a critical role for a conserved QLxxLR motif in Tn*3*-family TnpA transposase for binding the host DnaN processivity factor. We confirm and extend previous work indicating that Tn*3* family transposons bias transposition into plasmids and into the region of the host chromosome where DNA replication terminates. Multiple mutations with the QLxxLR motif that perturb the interaction with DnaN also perturb transposition *in vivo*, providing a functional link with target sites associated with DNA replication.

In the structural analysis of 12 representative TnpA proteins, the motif configurations present notable similarity to those found within Tn*4430* TnpA and a Tn*4430* TnpA-DNA complex. Common to these structures, the motifs are deeply embedded within DBD1, with only the hydrophilic side chain of the arginine residue in the QLxxLR motif distinctly extending from the DBD1 core to the protein surface. We speculate that DnaN might initially interact with the R59 position, but subsequently induce a conformational shift in Tn*1721* TnpA that in turn accommodates interactions with Q54 and L55. We favor a model where the interactions with DnaN helps deliver the TnpA transposase, but that DnaN is not a member of the final active transposition complex given the close proximity with amino acids used for DNA binding. For example, in the Tn*4430* TnpA structure H104 is predicted to interact with DNA but also has substantial non-covalent bond contacts with $Q55^{Tn4430}$ in both TnpA and TnpA-DNA complex structures (Figure 7B,C and Supplementary Figure S7).

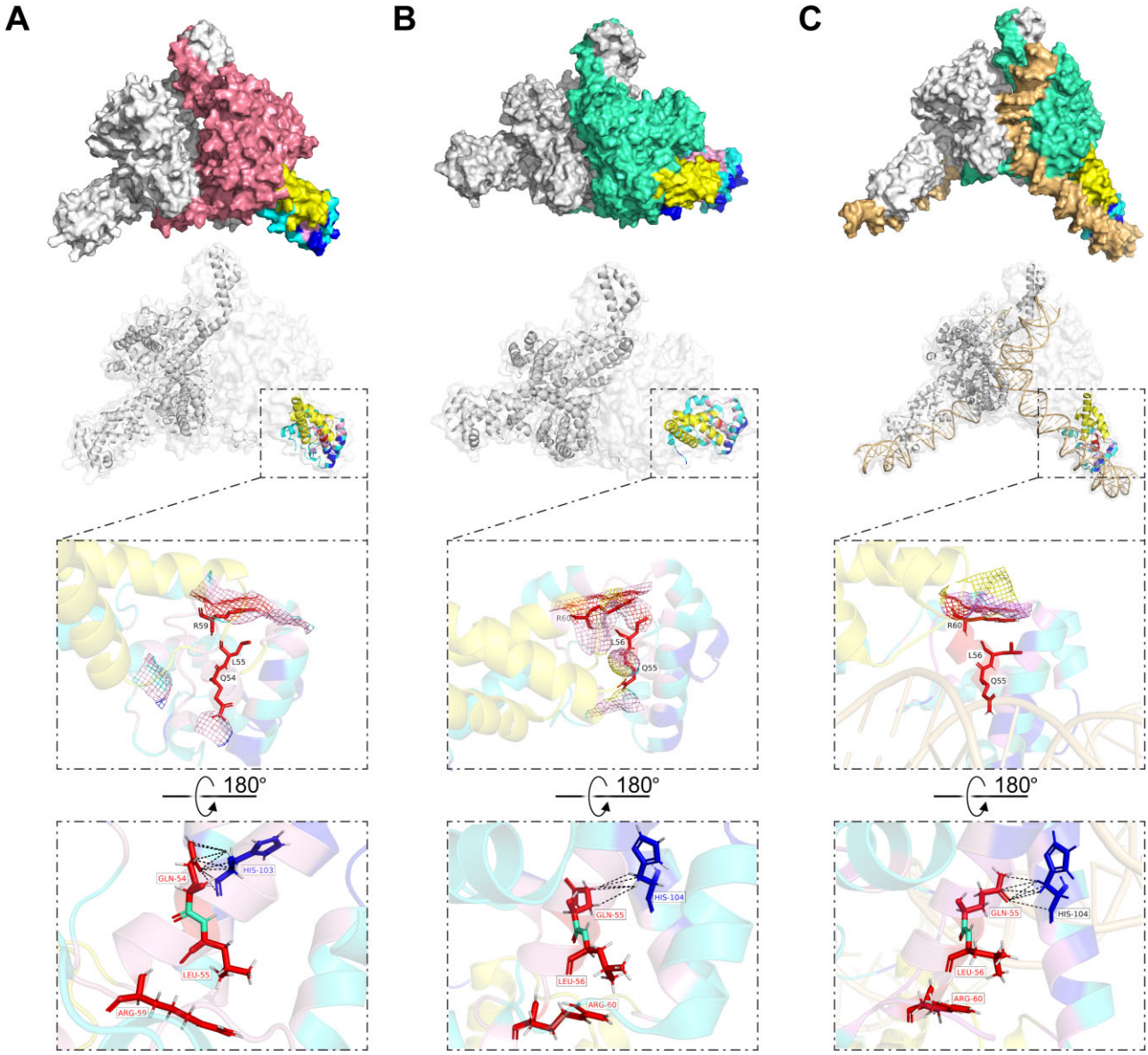

Figure 7. Structures of the DnaN-binding motif in TnpA and TnpA-DNA complex. (**A**) The structure map of the DnaN-binding motif in Tn*1721* TnpA. The chain A is colored in dark pink. In chain A, the DnaN-binding motif is colored in red, and the amino acids in close proximity to this motif, within a 5 Å radius is presented by pink. The DNA interacting amino acids are indicated by blue. The arm between DBD1 and DBD2 is colored in yellow. The remainder of the amino acids of DBD1 are indicated by cyan. (**B**) The structure map of the motif in Tn*4430* TnpA. The colors of protein are same with Tn*1721* TnpA, except for the chain A is colored in lime green. (**C**) The structure map of the motif in Tn4430 TnpA-DNA complex. The DNA is presented in beige. The mesh indicates the solvent-accessible surface of the key residues (Q54, L55, R59 in Tn*1721* and Q55, L56, R60 in Tn*4430*) in this motif, and the solvent-accessible surface of these residues defines the points of potential contacts between the motif and DnaN. The hydrogen bonds between glutamine (Q) of the QLxxLR motif and histidine (H) that was involved in TnpA DNA binding were indicated with dashed lines.

An analogous interaction was also identified in the dimeric Tn*1721* TnpA structure, where the Q54 is located within a predicted distance that could interact with H103 (Figure 7A and Supplementary Figure S7). Our genetics also suggests that only one clamp interacting motif is needed in a dimer of the TnpA transposase. While the TnpA (Q54A) protein is inactive for transposition on its own, it will allow robust transposition with a low level of expression of the TnpA (wt) proteins (Figure 4B and Supplementary Figure S4).

Interaction between TnpA and DnaN may be favored during the process of conjugation where leading and lagging strand synthesis occurs in the separate donor and recipient cells. A similar model has been suggested for the ability of transposon Tn*7* to target conjugal plasmids (46). When DNA replication terminates in the chromosome, DnaN may be uniquely available explaining how Tn*3* family transposons like Tn*917* and Tn*1721* bias transposition proximal to the most central chromosomal DNA replication termination site, *terC* (Figure 6B) (36,45). In a different transposon, Tn*7*, a dedicated target site identification protein, TnsE is used to interact with DnaN to help bias transposition to conjugal plasmids (11). Additional research will be needed to understand if TnsE and TnpA interact with DnaN in similar ways. Some group II mobile introns and IS*200*/IS*605* transposons also have an

interaction between their recombinase and DnaN (12,13). Some group II mobile introns benefit from using an interaction with DnaN to recognize the DNA template undergoing discontinuous DNA replication because it provides a 3′-OH to prime replication of the element. IS*200*/IS*605* transposons elements would benefit from targeting discontinuous DNA replication because they require single strand DNA as an integration target and for mobilization (12).

The TnpA expression plasmid was a highly preferred target in our mating-in assay (Figure 3B). The specific mechanism allowing transposition to be biased to the plasmid in this assay is unknown, but high levels of transcription in this vector could result in pervasive conflicts between transcription complexes and DNA replication forks. Conflicts that arise between highly transcribed genes and DNA replication are known to stall or perturb DNA replication, something that could make the processivity factor more available for an interaction with TnpA. A promoter and transcription terminator were hotspots for transposon targeting in the TnpA expression plasmid.

The QLxxLR motif is only found in specific subbranches within the Tn3 family elements indicating it was lost and acquired over time in certain lineages (Figure 1A-D and Supplementary Figure S1). The bacterial QLxxLR motif was originally identified in the five DNA polymerases and clamp loading components found in *E. coli* (42,47). While the QLxxLR motif interacts with a hydrophobic pocket in the DnaN protein, many other regions on DnaN have been identified as important for interaction with other proteins (48,49). The various surfaces that coordinate DnaN interactions at and outside the DNA replication fork help guide its many roles in DNA maintenance (50,51). Other mechanisms that allow a TnpA interaction with DnaN that do not involve a QLxxLR motif are likely to exist. This has been suggested for the IS*200*/IS*605* elements which have been shown to interact with DnaN but lack the QLxxLR motif (12). We suspect that TnpA examples that lack the QLxxLR motif are also likely to interact with the sliding clamp but dependent on other interaction regions of DnaN. Presence of the QLxxLR motif was often a function of the host where the element was found. The QLxxLR motif was common in Tn*3* TnpA representatives from Enterobacterales, Pseudomonadales and Aeromonadales (the motif was found in ∼60% of the TnpA examples) but rare in Lysobacterales and Kitasatosporales (<5%) (Figure 1D). The calculated KD of DnaN-TnpA interaction (∼0.29 μM) was higher than the KD reported for the interaction between DnaN and the δ subunit of the clamp loader (∼0.06 μM), suggesting a weaker interaction with TnpA. This feature is similar with most transposable elements (11,13), reflecting that transposable elements evolve to not interfere with interactions essential for normal activities of bacteria while maintaining the capacity of interacting with the host replication machinery for targeting transposition.

Here, we identify a conserved β-sliding clamp binding motif found across specific branches of Tn*3*-family TnpA transposase. This motif allows interaction between TnpA of Tn*3* family transposon Tn*1721* and DnaN. Such an interaction is essential for transposition. Our work unveils the mechanism whereby Tn*3* family transposons can bias transposition to replisomes through an interaction with the host replication machinery and reveals the general uniformity in targeting elements to DNA replication features across different types of transposons.

Data availability

The original data and code used in analysis that are not included in main text and supplementary materials have been uploaded to Mendeley Data (DOI:10.17632/hnmhh6w2st.4).

Supplementary data

Supplementary Data are available at NAR Online.

Acknowledgements

We would like to thank Dr Shan-Chi Hsieh for advice early in the project.

Author contributions: J.E.P. and Y.T. designed research; Y.T., J.Z., W.W. and W.L. performed research; J.G. performed biochemical analysis with help from H-Y.O.; M.T.P., W.L. and X.J. helped establish the experiment system at the early stages; Y.Z. and M.W. provided help to analyze the protein structures. All authors discussed the experiments and results; Y.T. and J.E.P. performed data analysis and prepared the manuscript with input from other authors. J.E.P., H-Y.O. and W.W. supervised the project.

Funding

National Natural Science Foundation of China [82002171]; Shanghai Sailing Program [20YF1444400]; USA National Institutes of Health [R01 GM129118, R35 GM152260]. Funding for open access charge: NSFC [82002171].

Conflict of interest statement

None declared.

References

1. Curcio,M.J. and Derbyshire,K.M. (2003) The outs and ins of transposition: from mu to kangaroo. *Nat. Rev. Mol. Cell Biol.*, **4**, 865–877.
2. Aziz,R.K., Breitbart,M. and Edwards,R.A. (2010) Transposases are the most abundant, most ubiquitous genes in nature. *Nucleic Acids Res.*, **38**, 4207–4217.
3. Nicolas,E., Lambin,M., Dandoy,D., Galloy,C., Nguyen,N., Oger,C.A. and Hallet,B. (2015) The Tn*3*-family of replicative transposons. *Microbiol. Spectr.*, **3**, https://doi.org/10.1128/microbiolspec.MDNA3-0060-2014.
4. Lima-Mendez,G., Oliveira Alvarenga,D., Ross,K., Hallet,B., Van Melderen,L., Varani,A.M. and Chandler,M. (2020) Toxin-antitoxin gene pairs found in Tn*3* family transposons appear to be an integral part of the transposition module. *mBio*, **11**, e00452-20.
5. Cuzon,G., Naas,T. and Nordmann,P. (2011) Functional characterization of Tn*4401*, a Tn*3*-based transposon involved in *bla*$_{KPC-2}$ gene mobilization. *Antimicrob. Agents Chemother.*, **55**, 5370–5373.
6. Tang,Y., Li,G., Liang,W., Shen,P., Zhang,Y. and Jiang,X. (2017) Translocation of carbapenemase gene *bla*$_{KPC-2}$ both internal and external to transposons occurs via novel structures of Tn*1721* and exhibits distinct movement patterns. *Antimicrob. Agents Chemother.*, **61**, e01151-17.
7. Tang,Y., Li,G., Shen,P., Zhang,Y. and Jiang,X. (2022) Replicative transposition contributes to the evolution and dissemination of KPC-2-producing plasmid in Enterobacterales. *Emerg. Microbes Infect.*, **11**, 113–122.

8. Kretschmer,P.J. and Cohen,S.N. (1977) Selected translocation of plasmid genes: frequency and regional specificity of translocation of the Tn*3* element. *J. Bacteriol.*, **130**, 888–899.
9. Muster,C.J. and Shapiro,J.A. (1981) Recombination involving transposable elements: on replicon fusion. *Cold Spring Harb. Symp. Quant. Biol.*, **45**, 239–242.
10. Nicolas,E., Oger,C.A., Nguyen,N., Lambin,M., Draime,A., Leterme,S.C., Chandler,M. and Hallet,B.F. (2017) Unlocking Tn*3*-family transposase activity in vitro unveils an asymetric pathway for transposome assembly. *Proc. Natl. Acad. Sci. U.S.A.*, **114**, E669–E678.
11. Parks,A.R., Li,Z.P., Shi,Q.J., Owens,R.M., Jin,M.M. and Peters,J.E. (2009) Transposition into replicating DNA occurs through interaction with the processivity factor. *Cell*, **138**, 685–695.
12. Lavatine,L., He,S., Caumont-Sarcos,A., Guynet,C., Marty,B., Chandler,M. and Ton-Hoang,B. (2016) Single strand transposition at the host replication fork. *Nucleic Acids Res.*, **44**, 7866–7883.
13. Garcia-Rodriguez,F.M., Neira,J.L., Marcia,M., Molina-Sanchez,M.D. and Toro,N. (2019) A group II intron-encoded protein interacts with the cellular replicative machinery through the beta-sliding clamp. *Nucleic Acids Res.*, **47**, 7605–7617.
14. Lopez de Saro,F.J., Georgescu,R.E., Goodman,M.F. and O'Donnell,M. (2003) Competitive processivity-clamp usage by DNA polymerases during DNA replication and repair. *EMBO J.*, **22**, 6408–6418.
15. Johnson,A. and O'Donnell,M. (2005) Cellular DNA replicases: components and dynamics at the replication fork. *Annu. Rev. Biochem.*, **74**, 283–315.
16. Taylor,M.S., LaCava,J., Mita,P., Molloy,K.R., Huang,C.R., Li,D., Adney,E.M., Jiang,H., Burns,K.H., Chait,B.T., *et al.* (2013) Affinity proteomics reveals human host factors implicated in discrete stages of LINE-1 retrotransposition. *Cell*, **155**, 1034–1048.
17. Mita,P., Wudzinska,A., Sun,X., Andrade,J., Nayak,S., Kahler,D.J., Badri,S., LaCava,J., Ueberheide,B., Yun,C.Y., *et al.* (2018) LINE-1 protein localization and functional dynamics during the cell cycle. *eLife*, **7**, e30058.
18. O'Leary,N.A., Wright,M.W., Brister,J.R., Ciufo,S., Haddad,D., McVeigh,R., Rajput,B., Robbertse,B., Smith-White,B., Ako-Adjei,D., *et al.* (2016) Reference sequence (RefSeq) database at NCBI: current status, taxonomic expansion, and functional annotation. *Nucleic Acids Res.*, **44**, D733–D745.
19. Mistry,J., Chuguransky,S., Williams,L., Qureshi,M., Salazar,G.A., Sonnhammer,E.L.L., Tosatto,S.C.E., Paladin,L., Raj,S., Richardson,L.J., *et al.* (2021) Pfam: the protein families database in 2021. *Nucleic Acids Res.*, **49**, D412–D419.
20. Finn,R.D., Clements,J., Arndt,W., Miller,B.L., Wheeler,T.J., Schreiber,F., Bateman,A. and Eddy,S.R. (2015) HMMER web server: 2015 update. *Nucleic Acids Res.*, **43**, W30–W38.
21. Grant,C.E., Bailey,T.L. and Noble,W.S. (2011) FIMO: scanning for occurrences of a given motif. *Bioinformatics*, **27**, 1017–1018.
22. Schoch,C.L., Ciufo,S., Domrachev,M., Hotton,C.L., Kannan,S., Khovanskaya,R., Leipe,D., McVeigh,R., O'Neill,K., Robbertse,B., *et al.* (2020) NCBI Taxonomy: a comprehensive update on curation, resources and tools. *Database (Oxford)*, **2020**, baaa062.
23. Winter,D.J. (2017) rentrez: an R package for the NCBI eUtils API. *R Journal*, **9**, 520–526.
24. Katoh,K. and Standley,D.M. (2013) MAFFT multiple sequence alignment software version 7: improvements in performance and usability. *Mol. Biol. Evol.*, **30**, 772–780.
25. Waterhouse,A.M., Procter,J.B., Martin,D.M., Clamp,M. and Barton,G.J. (2009) Jalview Version 2–a multiple sequence alignment editor and analysis workbench. *Bioinformatics*, **25**, 1189–1191.
26. Price,M.N., Dehal,P.S. and Arkin,A.P. (2010) FastTree 2–approximately maximum-likelihood trees for large alignments. *PLoS One*, **5**, e9490.
27. Letunic,I. and Bork,P. (2021) Interactive Tree Of Life (iTOL) v*5*: an online tool for phylogenetic tree display and annotation. *Nucleic Acids Res.*, **49**, W293–W296.
28. Crooks,G.E., Hon,G., Chandonia,J.M. and Brenner,S.E. (2004) WebLogo: a sequence logo generator. *Genome Res.*, **14**, 1188–1190.
29. Wang,M., Goh,Y.X., Tai,C., Wang,H., Deng,Z. and Ou,H.Y. (2022) VRprofile2: detection of antibiotic resistance-associated mobilome in bacterial pathogens. *Nucleic Acids Res.*, **50**, W768–W773.
30. Sibley,M.H. and Raleigh,E.A. (2012) A versatile element for gene addition in bacterial chromosomes. *Nucleic Acids Res.*, **40**, e19.
31. Wu,Y., Li,Q. and Chen,X.Z. (2007) Detecting protein-protein interactions by Far western blotting. *Nat. Protoc.*, **2**, 3278–3284.
32. Peters,J.E. and Craig,N.L. (2001) Tn7 recognizes transposition target structures associated with DNA replication using the DNA-binding protein TnsE. *Genes Dev.*, **15**, 737–747.
33. Pei,T.T., Kan,Y., Wang,Z.H., Tang,M.X., Li,H., Yan,S., Cui,Y., Zheng,H.Y., Luo,H., Liang,X., *et al.* (2022) Delivery of an Rhs-family nuclease effector reveals direct penetration of the gram-positive cell envelope by a type VI secretion system in *Acidovorax citrulli*. *mLife*, **1**, 66–78.
34. Battesti,A. and Bouveret,E. (2012) The bacterial two-hybrid system based on adenylate cyclase reconstitution in *Escherichia coli*. *Methods*, **58**, 325–334.
35. Xue,T., Zhao,L., Sun,H., Zhou,X. and Sun,B. (2009) LsrR-binding site recognition and regulatory characteristics in *Escherichia coli* AI-2 quorum sensing. *Cell Res.*, **19**, 1258–1268.
36. Garsin,D.A., Urbach,J., Huguet-Tapia,J.C., Peters,J.E. and Ausubel,F.M. (2004) Construction of an *Enterococcus faecalis* Tn*917*-mediated-gene-disruption library offers insight into Tn*917* insertion patterns. *J. Bacteriol.*, **186**, 7280–7289.
37. Burley,S.K., Bhikadiya,C., Bi,C., Bittrich,S., Chao,H., Chen,L., Craig,P.A., Crichlow,G.V., Dalenberg,K., Duarte,J.M., *et al.* (2023) RCSB Protein Data Bank (RCSB.org): delivery of experimentally-determined PDB structures alongside one million computed structure models of proteins from artificial intelligence/machine learning. *Nucleic Acids Res.*, **51**, D488–D508.
38. Jumper,J., Evans,R., Pritzel,A., Green,T., Figurnov,M., Ronneberger,O., Tunyasuvunakool,K., Bates,R., Zidek,A., Potapenko,A., *et al.* (2021) Highly accurate protein structure prediction with AlphaFold. *Nature*, **596**, 583–589.
39. Sievers,F. and Higgins,D.G. (2021) The clustal omega multiple alignment package. *Methods Mol. Biol.*, **2231**, 3–16.
40. Eddy,S.R. (2004) Where did the BLOSUM62 alignment score matrix come from? *Nat. Biotechnol.*, **22**, 1035–1036.
41. Nagar,N., Ben Tal,N. and Pupko,T. (2022) EvoRator: prediction of residue-level evolutionary rates from protein structures using machine learning. *J. Mol. Biol.*, **434**, 167538.
42. Dalrymple,B.P., Kongsuwan,K., Wijffels,G., Dixon,N.E. and Jennings,P.A. (2001) A universal protein-protein interaction motif in the eubacterial DNA replication and repair systems. *Proc. Natl. Acad. Sci. U.S.A.*, **98**, 11627–11632.
43. Shkumatov,A.V., Aryanpour,N., Oger,C.A., Goossens,G., Hallet,B.F. and Efremov,R.G. (2022) Structural insight into Tn3 family transposition mechanism. *Nat. Commun.*, **13**, 6155.
44. Georgescu,R.E., Kim,S.S., Yurieva,O., Kuriyan,J., Kong,X.P. and O'Donnell,M. (2008) Structure of a sliding clamp on DNA. *Cell*, **132**, 43–54.
45. Shi,Q., Huguet-Tapia,J.C. and Peters,J.E. (2009) Tn*917* targets the region where DNA replication terminates in *Bacillus subtilis*, highlighting a difference in chromosome processing in the firmicutes. *J. Bacteriol.*, **191**, 7623–7627.
46. Peters,J.E. (2014) Tn*7*. *Microbiol. Spectr.*, **2**, https://doi.org/10.1128/microbiolspec.MDNA3-0010-2014.
47. Jeruzalmi,D., Yurieva,O., Zhao,Y., Young,M., Stewart,J., Hingorani,M., O'Donnell,M. and Kuriyan,J. (2001) Mechanism of processivity clamp opening by the delta subunit wrench of the

clamp loader complex of *E. coli* DNA polymerase III. *Cell*, **106**, 417–428.
48. Heltzel,J.M., Maul,R.W., Scouten Ponticelli,S.K. and Sutton,M.D. (2009) A model for DNA polymerase switching involving a single cleft and the rim of the sliding clamp. *Proc. Natl. Acad. Sci. U.S.A.*, **106**, 12664–12669.
49. Sutton,M.D. and Duzen,J.M. (2006) Specific amino acid residues in the beta sliding clamp establish a DNA polymerase usage hierarchy in *Escherichia coli*. *DNA Repair (Amst.)*, **5**, 312–323.
50. Kath,J.E., Chang,S., Scotland,M.K., Wilbertz,J.H., Jergic,S., Dixon,N.E., Sutton,M.D. and Loparo,J.J. (2016) Exchange between *Escherichia coli* polymerases II and III on a processivity clamp. *Nucleic Acids Res.*, **44**, 1681–1690.
51. Pillon,M.C., Babu,V.M., Randall,J.R., Cai,J., Simmons,L.A., Sutton,M.D. and Guarne,A. (2015) The sliding clamp tethers the endonuclease domain of MutL to DNA. *Nucleic Acids Res.*, **43**, 10746–10759.

Received: March 1, 2024. **Revised:** July 18, 2024. **Editorial Decision:** July 19, 2024. **Accepted:** July 23, 2024